한국지구시스템공학회지
Vol. 42, No. 5 (2005) pp. 485-497

연구논문

Reviews of hydrothermal gold-silver mineralization at the Mugeuk deposit, Korea : A geochemical study

Chul-Ho Heo and Jae-Ho Lee*

무극 광상의 열수 금-은 광화작용 : 지구화학적 연구 재고찰

허철호[1] · 이재호[2]*

요 약 : 무극광산은 남한에서 역사적으로 가장 큰 금-은 생산지였으며, 평균품위 약 8g/ton의 금광석을 천만톤 이상 생산했었다. 본 광상은 쥬라기 화강섬록암과 백악기 석영반암내 발달한 단층과 열극을 충진하는 10개조 이상의 석영-방해석맥으로 구성되어 있다. 본 광상의 광맥은 백악기 후기 6회의 연속적인 열수활동 중 형성되었다. 맥내 광석광물의 조성은 복잡하며, 주로 에렉트럼(23-51 atom. % Au)을 수반한 황철석과 천금속 황화물, 자연은, 휘은석과 은황화염이 산출된다. 광화 1기 맥은 금과 은을 배태하지 않고, 광화 2기에서 5기 동안에는, 상당량의 금과 은이 침전되었다. 광화 3기와 4기는 뚜렷한 황화물대에서 금침전이 활발한 반면에, 광화 5기는 은 침전이 지배적이었다. 광화 6기 맥은 광화후기의 barren한 석영-방해석-형석으로 구성되어 있다. 다양한 지구화학적 자료에 의하면, 금과 은의 침전은 주로 광화유체의 냉각 및 희석작용에 의해서 야기되었으며, 열수계로 연속적인 천수가 유입되었다. 유체포유물 자료에 의하면, 광학작용이 진행되면서 온도와 염농도의 일반적인 감소를 보여준다. 광석광물 조합은 금과 은이 침전하는 동안 온도가 감소하면서 황분압의 감소를 지시한다. 열수유체의 산소안정동위원소 값은 광화 2기에서 6기로 진행하면서 +3.0 ~ -7.4‰ 까지 감소하고, 수소안정동우원소값의 범위는 -66 ~ -84‰이다. 따라서, 광물조성, 금/은비, 유체지구화학 관점에서 고려할 때, 무극 금-은광상은 화강암을 모암으로 열수계에 일시적인 천수 유입의 결과로 생성되었을 것으로 사료된다.

주요어 : 무극광산, 금-은광화작용, 유체포유물, 산소, 수소 안정동위원소

Abstract : The Mugeuk mine was historically the largest gold-silver producer in South Korea, and yielded more than ten metric tons of gold with an average grade of about 8 g/ton Au . Ore deposits consist of more than 10 subparallel quartz-calcite veins that fill faults and fractures in Jurassic granodiorite and Cretaceous quartz porphyry. Veins formed during six successive hydrothermal events of Late Cretaceous age. Ore mineralogy of the veins is complex, consisting mainly of base-metal sulfides with electrum (23-51 atom. % Au), native silver, argentite and silver sulfosalts. Stage I veins do not contain gold and silver minerals. During stages II to V, economic quantities of gold and silver were precipitated. Stages III and IV represent the culmination of gold precipitation in distinct sulfide bands, whereas stage V represents a shift to dominantly silver deposition. Stage VI veins are post-ore barren quartz-calcite-fluorite. A variety of types of geochemical data indicate that deposition of gold and silver resulted mainly from cooling and mixing of ore fluids, accompanying successive incursions of meteoric water into the hydrothermal system. Fluid inclusion data show general decreases of temperature and salinity within each stage. Ore mineral assemblages indicate decreases in the fugacity of sulfur with decreasing temperatures during the deposition of gold and silver. Measured and calculated $\delta^{18}O$ values of hydrothermal fluids decrease generally from +3.0 to 7.4‰ from stages II through VI, and δ D values range from 66 to 84‰. The Au-Ag deposits at Mugeuk, in particular, mineralogy, Au/Ag ratios and fluid geochemistry, are the result of episodic meteoric water events within the granite-hosted hydrothermal system.

Key words : Mugeuk mine, Gold-silver mineralization, Fluid inclusion, Oxygen, Hydrogen stable isotope

Introduction

Most gold-silver vein deposits in Korea are intimately associated with major periods of Jurassic and Cretaceous granitic plutonism (Shimazaki *et al.*, 1986). Cretaceous granites have been shown to be higher level intrusions (<2-3 km) than Jurassic granites (>5 km, Tsusue *et al.*, 1981), providing an opportunity to investigate the influence of depth of emplacement on the post-magmatic evolution of granite-related gold systems. Three main types of deposits have been documented previously, and these display a consistent relationship among depth, water-to-rock ratio, and Au/Ag

2005년 4월 27일 접수, 2005년 9월 15일 채택
1) 국립공원관리공단 국립공원연구소
2) 한국지질자원연구원 지질기반정보부
*Corresponding Author(이재호)
E-mail: ihlee@kigam.re.kr
Address; Geology & Geoinformation Division, Korea Institute of Geoscience and Mineral Resources, 305-350, Korea

ratio: gold-rich mesothermal gold deposits; Korean- type gold-silver; and more silver-rich epithermal deposits (Shelton *et al*., 1988).

Mesothermal deposits have not been frequently reported or studied in Korea (Shelton *et al*., 1988; So *et al*., 1995), compared with other types of gold-silver vein deposits. They appear to be associated genetically with Jurassic granites (Lee, 1981) and are characterized by high Au/Ag ratios (5:1-8:1). Geochemical studies of these deposits indicate that gold deposition occurred at temperatures of 300° to 370℃ in response to unmixing of CO_2-rich fluids at depths of >4.5 km (Shelton *et al*., 1988; So *et al*., 1995). Korean-type deposits are associated with Late Jurassic-Early Cretaceous granites (Lee, 1981) and are characterized by moderately high Au/Ag ratios (1:5-2:1) and a general paucity of sulfide minerals (Sugaki *et al*., 1986). Geochemical studies of Korean-type gold-silver deposits indicate that gold deposition occurred at temperatures near 270℃ in response to boiling and cooling at depths around 1.25 km (So *et al*., 1987). The more silver-rich epithermal deposits are associated genetically with Late Cretaceous-Tertiary granites and are characterized by low Au/Ag ratios (1:10-1:200) and more abundant, complex sulfide mineralization. Geochemical studies of these deposits indicate that gold-silver deposition occurred at temperatures of <240℃ in response to boiling and cooling at depths of <0.75 km (Shelton *et al*., 1990).

The Mugeuk district's gold-silver deposits are located approximately 80 km southeast of Seoul (Fig. 1) and historically have been the most productive gold-silver deposits in Korea. Within this district, several mines are closely spaced (Fig. 2). The Mugeuk mine has been exploited for gold and silver since 1934, and produced about 10 metric tons of gold and 48 metric tons of silver during the peak production from 1986 to 1996 from ore with average grades of 7.8 g/ton Au and 40 g/ton Ag. Its deposits are comprised of several fissure-filling quartz-calcite veins within a middle Jurassic porphyritic granodiorite. Of these veins, the Samhyeongje vein (Fig. 2) was mined most recently, until May 1998.

Several previous investigators have studied the geology of the mining district and the physicochemical conditions of its ore mineralization. Shin and Suh (1987) documented the history of exploration and

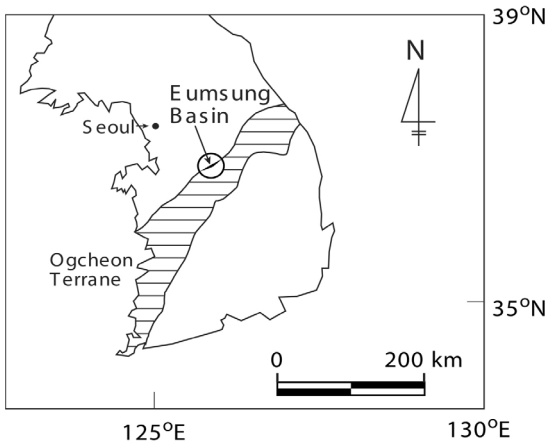

Fig. 1. Index map of the Korean Peninsula showing location of the Cretaceous Eumsung Basin and the Ogcheon Terrane.

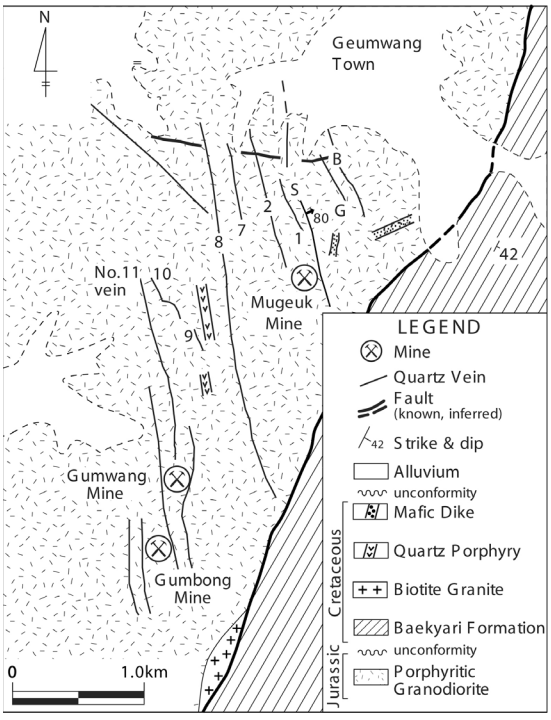

Fig. 2. Geologic map of the Mugeuk Au-Ag mine area. The numbers are the names of mineralized veins. B = Baksan Vein, G = Geumyong Vein, S = Samhyeongje Vein.

development of the Mugeuk gold-silver mine, and described the general geology and the ore characteristics

of its deposits. Park and Kang (1988) studied the mineralogy of the Mugeuk ores. Kim *et al.* (1990) performed a reconnaissance fluid inclusion and sulfur isotope study of the Samhyeongje vein of the Mugeuk mine, but the results of the study were based on a few (<10) unconstrained samples collected only from an ore dressing plant at surface and, therefore, could not cover the whole range of underground mine workings. The Mugeuk deposits are not readily classified as either "Korean-type" or epithermal type goldsilver deposits. Our present study focuses mainly on the most recently mined Samhyeongje vein and elucidates the relationship between its ore mineralogy and the geochemistry of this hydrothermal system.

Geologic Setting

The Mugeuk gold-silver deposits occur within the Eumsung Basin (Yang and Chang, 1987; Fig. 1), one of several small, fault-bounded Cretaceous sedimentary basins developed along the northern border of the Ogcheon Terrane, an orogenic belt containing Cambrian through Jurassic age rocks (Kim, 1987). The Eumsung Basin is approximately 45×10 km in size and is elongated in a SW-NE direction, parallel to the extensional direction of the Ogcheon Terrane (Fig. 1; Cheong *et al.*, 1976). The geology of this mining area is relatively simple and consists of Jurassic to Cretaceous granitic intrusions and Cretaceous sedimentary rocks (Shin and Suh, 1987). Granitic rocks comprise porphyritic granodiorite, quartz porphyry and biotite granite with minor mafic dikes (Fig. 2).

Porphyritic granodiorite characterized by large microcline phenocrysts hosts the Mugeuk mine. Quartz, microcline, orthoclase, plagioclase and biotite are the main minerals in the granodiorite, along with minor muscovite, hornblende and sphene. The porphyritic granodiorite displays plagioclase compositional zoning and myrmekitic textures. Our K-Ar analysis of igneous biotite yields a date of 186±10 Ma. The Cretaceous Baekyari Formation consists mainly of pebbly sandstone, shale, sandy shale and conglomerate. The sedimentary rocks strike N25–45°E with dips of 30–50°SE and are in fault contact with the Jurassic porphyritic granodiorite. The fault strikes N20°E and dips 70–80°SE (Shin and Suh, 1987). Other minor faults strike N70–80°W and dip 70–80°SW, and these may have been conduits for ore-forming fluids.

A small biotite granite stock intruded along the boundary between the porphyritic granodiorite and the Baekyari Formation in the southern part of the mining district (Fig. 2). This stock is composed mainly of orthoclase, plagioclase, quartz and biotite. Also, a quartz porphyry dike intruded the porphyritic granodiorite, parallel to the gold- and silver-bearing quartz veins.

Ore Veins

The Mugeuk deposits are comprised of several hydrothermal quartz-calcite veins that fill fractures developed along a N10° to 15°W-trending and 70° to 85°NE-dipping fault zone within the Jurassic granodiorite. The mineralized veins are named the Baksan, Geumyong, Samhyeongje, No. 1, No. 2, No. 7, No. 8, No. 9, No. 10 and No. 11 veins (Shin and Suh, 1987). Ore veins extend discontinuously 400 to 2,000 m on surface, and for as much as 800 m vertically with average widths of about 1 m or less. Ore veins pinch and swell, and vein textures include brecciation, crustification and banding, indicating repeated fracturing and rehealing. Ore veins show distinct textural and compositional variations with depth. In the shallow parts of veins, massive quartz and sulfides are common, and silver-bearing minerals such as argentite and native silver are more abundant. At depth, brecciation and banded textures dominate, and gold content of electrum increases. Ore shoots with average gold grades of about 100 g/t are developed along swells that are characterized by brecciation and sulfide banding textures.

Hydrothermal alteration of wallrock granodiorite occurs in several tens of meter-wide envelopes whose widths are typically proportional to vein thickness. The alteration envelopes are characterized by overlapping sericitic (inner), chloritic, and propylitic (outer) zones, each with trace disseminated pyrite. The sericitic zone is generally less than 3 m from vein margins and is greenish-white in color and consists of sericite, lesser chlorite, smectite and pyrite; there has been a complete

destruction of biotite and hornblende. About 70 to 90% of the plagioclase was altered to sericite and smectite. Twinning of plagioclase and K-feldspar crystals in the sericitic alteration zone is obliterated. Chloritic alteration consists of dominant chlorite, sericite and pyrite with residual biotite. About 20 to 70% of the plagioclase and K-feldspar have been altered to sericite. The propylitic alteration zone is very wide (extending as far as 40 m from vein margins) and consists of an epidote and chlorite alteration of biotite and hornblende. A hydrothermal sericite yielded a K-Ar date of 98 ±5 Ma (Shimazaki *et al.*, 1986).

Mineralogical Paragenesis

For the present study, we examined ninety-seven vein samples collected from underground ore stopes during the period 1987 to 1997. Our sample suite covers nearly the whole range of underground mine workings both horizontally and vertically. Based on careful investigation of mineral assemblages, textural and crosscutting relationships of veins, and microscopic study of ore samples, we have divided the hydrothermal Au-Ag mineralization into six stages at the Mugeuk mine (Fig. 3). Ore mineral compositions were determined by electron microprobe in this study. Analyses of electrum, sphalerite and arsenopyrite are available as electronic supplements.

Stage I mineralization consists of early chalcedonic quartz and later milky quartz with euhedral pyrite. Early, light-green colored chalcedonic quartz contains wall-rock fragments that have been altered to sericite and chlorite. Chalcedonic quartz has planar contacts with later milky quartz that contains rare disseminated subhedral to euhedral pyrites up to 2 mm in diameter. Stage I veins are crosscut by stage II veins of dark gray quartz.

Stage II mineralization comprises gray quartz, arsenopyrite, base-metal sulfide minerals, electrum and minor hematite. Sulfide minerals usually constitutes less than 5 vol % of stage II mineralization. Early dark gray quartz is, in part, chalcedonic and contains disseminated arsenopyrite and other sulfide minerals. Wall-rock fragment inclusions in gray quartz are characteristically altered to sericite. Late gray quartz

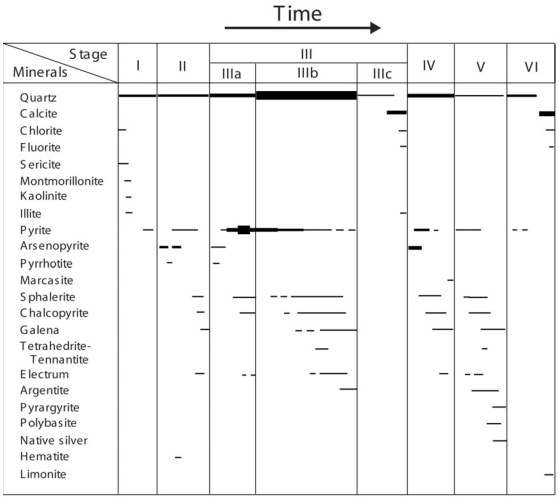

Fig. 3. Vein mineral paragenesis of the Mugeuk Au-Ag deposits. Thickness of lines corresponds to relative abundance of minerals.

commonly displays vuggy textures in the central portions of the vein. Fine-grained, euhedral arsenopyrite (avg. 31.1-32.2 atomic % As) contains tiny inclusions of pyrrhotite and hematite and occurs as disseminations together with pyrite. Arsenopyrite is surrounded by, and fractures within it are filled with, electrum, sphalerite, and galena. Pyrite occurs as coarse-grained clusters of cubes and as intergrowths with arsenopyrite. Pyrite commonly contains small rounded inclusions of base-metal sulfide minerals and electrum. Electrums (46.7-47.7 atomic % Au) are commonly associated with sphalerites (1.5-1.9 mole % FeS), and also occurs as tiny blebs with sphalerite and galena within pyrite and arsenopyrite and/or filling narrow fractures in arsenopyrite.

Stage III was the main gold mineralizing period and was characterized by deposition of sulfide bands, brecciation, and the precipitation of pale pink to white quartz. Based on mineral assemblages and textures, this stage can be divided into three substages. Minerals of stage IIIa include arsenopyrite, pyrrhotite, pyrite, sphalerite, chalcopyrite and electrum as distinct sulfide bands with white quartz along vein margins. Sulfide bands occupy more than 60 vol. % of a typical stage IIIa vein. Abundant subhedral pyrite occurs as sulfide bands with arsenopyrite (29.4-32.6 atomic % As) incl-

uding inclusions of sphalerite and electrum. Sphalerite (1.4-3.5 mole % FeS) is associated with electrum and chalcopyrite, and often shows chalcopyrite disease texture. Electrum (39.0-50.9 atomic % Au) occurs as tiny blebs within pyrite and arsenopyrite. Monoclinic pyrrhotite occurs as inclusions within arsenopyrite. Stage IIIb was the major gold depositing stage and occurs in the center of stage III veins. Pyrite, sphalerite, chalcopyrite, galena, argentite, electrum and tetrahedritetennantite in the form of aggregates and/or disseminations within pink white quartz comprise the minerals of stage IIIb. Sulfide minerals constitute about 10 to 20 vol. % of stage IIIb mineralization. Subhedral to euhedral pyrite is commonly associated with electrum and base-metal sulfide minerals, and contains inclusions of electrum, argentite, sphalerite, chalcopyrite and galena. Pyrite was partly replaced by sphalerite, chalcopyrite, galena and supergene limonite. Subhedral sphalerite occurs together with pyrite, chalcopyrite, galena and electrum. It also infills fractures in earlier pyrite and arsenopyrite and partly replaces those minerals along grain boundaries. Sphalerite is black in color, but its iron content is low (0.2-2.9 mole % FeS). Electrum (32.1-43.1 atomic % Au) ranging from 1 to 500 μm in grain size (avg. 50 μm) is closely associated with sphalerite, galena, chalcopyrite and argentite. It occurs as small blebs within pyrite and sphalerite, and together with chalcopyrite and galena fills the interstices among pyrite grains. Barren stage IIIc veins cut stage IIIb veins and are comprised of clear quartz, calcite, fluorite, chlorite and illite.

Stage IV veins cut earlier stage III veins and are comprised of gray quartz, arsenopyrite, pyrite, sphalerite, chalcopyrite, galena, marcasite and electrum. Sulfides comprise about 15% by volume of stage IV minerals. This stage is characterized by the occurrence of coarse-grained aggregates of arsenopyrite (28.4-33.1 atomic % As) that are associated with pyrite, sphalerite (1.2-9.5 mole % FeS) and chalcopyrite. Arsenopyrite also contains inclusions of electrum, chalcopyrite, sphalerite and galena. Electrum (46.3-47.2 atomic % Au) is associated commonly with sphalerite, chalcopyrite and galena, and fills the fractures within arsenopyrite and pyrite. Marcasite replaces pyrite and arsenopyrite.

Stage V is the main silver-depositing stage and is comprised of narrow veinlets and/or numerous microfracture-fillings within earlier stage IIIb quartz. Ore minerals comprising over 80 vol % of stage V vein include pyrite, sphalerite, chalcopyrite, galena, argentite, electrum, native silver, polybasite, pyrargyrite and tetrahedrite. Minor (<20 vol %) clear quartz occurs as gangue. Sphalerite (0.3-2.9 mole % FeS) is associated with pyrite, chalcopyrite, galena and electrum. Electrum (23.3-24.9 atomic % Au) fills microfractures and occurs as tiny blebs within euhedral pyrite and is often replaced by native silver and argentite. Argentite is associated with electrum, native silver and polybasite. Polybasite is the most abundant silver-sulfosalt and is associated with argentite, pyrargyrite and native silver.

Stage VI veins crosscut all the previous stages and consist principally of clear quartz, pyrite, calcite and fluorite but contain no ore minerals. Calcite and fluorite also fill vugs with chlorite in the central part of stage VI veins.

Fluid inclusion study

Fluid inclusions within 73 samples of quartz, calcite and sphalerite were examined microthermometrically, using a Fluid Inc. gasflow heating/freezing system, in order to determine the temperatures of mineral precipitation and compositions of hydrothermal fluids, and to document any variations with time.

Quartz samples from the Mugeuk mine contain abundant fluid inclusions that probably formed during repeated fracturing and healing, both during and after quartz deposition. It is commonly difficult or impossible to distinguish primary, pseudosecondary and secondary inclusions in these samples using the criteria of Roedder (1984). Shelton and Orville (1980) has shown in crack-healing experiments with quartz that one of the final stages in annealing of fractures is the transformation of flat island-like inclusions into isolated, regularly shaped inclusions. These inclusions may then migrate away from the healed fracture surfaces and have the appearance of primary inclusions. Due to the inherent difficulty of distinguishing between pseudosecondary and true primary inclusions, in our study we have employed a more practical distinction

between primary + pseudosecondary (P+PS) inclusions and secondary (S) inclusions.

Based on the number and relative volume proportions of phases at 25°C, only one type of fluid inclusion was found. The inclusions are water-rich, two-phase inclusions with a vapor bubble comprising 5 to 25 volume percent, and typically averaging 10 vol %. Rare inclusions containing vapor bubbles of 45 vol % occur in stage IV milky quartz. Fluid inclusions vary in size from <2 to about 50 μm (avg. 510 μm). The inclusions contain no daughter minerals, and CO_2 was not detected during freezing experiments or by crushing.

Homogenization temperatures and salinities

Figures 4 and 5 show the ranges of homogenization temperatures and salinities for inclusions in vein minerals, respectively. Homogenization temperatures (T_h) and final ice melting temperatures have standard errors of ±1.0° and ±0.2°C, respectively. Salinity data for inclusions are based on freezing point depression in the system H_2O-NaCl (Bodnar, 1993).

T_h values were determined for 938 fluid inclusions in minerals from all six mineralization stages of the Mugeuk mine. Within the histograms of T_h values for primary and pseudosecondary inclusions (Fig. 4) are three notable trends, corresponding to the early stages (I and II), the main gold-silver depositing stage III, and later silver- and post-ore stages (IV through VI). Fluid inclusions from pre-main-gold stages I and II have similar maximum T_h values of about 310°C. Within the main gold-depositing stage III, there is a cooling trend recorded by apparent decreases in both maximum (365 to 290°C) and average (300 to 230°C) T_h values with time from stage IIIa through IIIc. By the advent of stage IV, average T_h values increase again to near 250°C and decrease again through silver-rich stage V and post-ore stage VI.

Fluid inclusions within stage I, II, IIIa, and IV quartz were too small for reliable determination of fluid salinity. Histograms of the 160 salinity determinations from the other stages of the paragenesis indicate two notable patterns corresponding to the main gold ore deposition and post-gold ore stages (Fig. 5). Maximum (7.5 to 5.0 wt. % equiv. NaCl) and average (5.0 to 3.0 wt. % equiv. NaCl) fluid salinities decreased with time

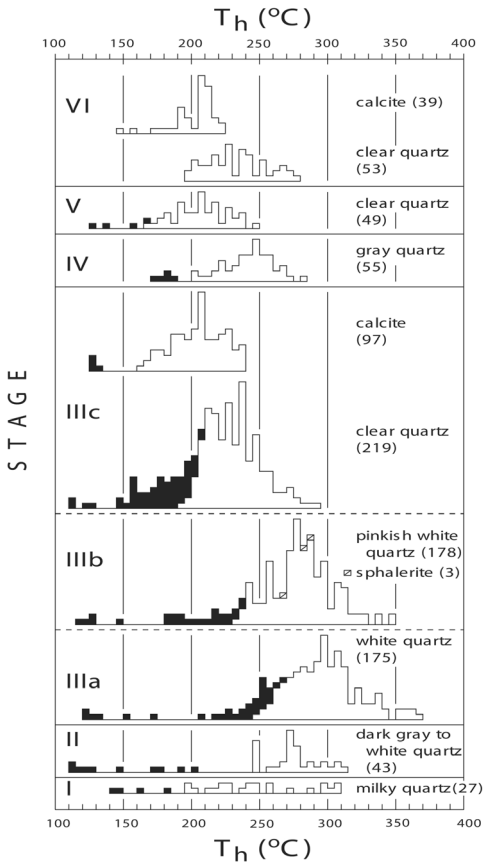

Fig. 4. Histograms of homogenization temperatures (T_h) of fluid inclusions in vein minerals of the Mugeuk Au-Ag mine. Data in black are for secondary inclusions; unfilled are for primary + pseudosecondary inclusions. Numbers in parentheses beside mineral names indicate the number of inclusions measured.

during the main gold-depositing stages (stages IIIb and c). Average fluid salinities decreased (5.0 to 2.2 wt. % equiv. NaCl) during silver-ore stage V and post-ore stage VI quartz and calcite deposition.

Variations in temperature and composition of hydrothermal fluids

The differences between minimum and maximum T_h values of P+PS inclusions within each of the six paragenetic stages were quite large (Fig. 4) and could, in part, be due to variability of pressure conditions during hydrofracturing and fluid entrapment. For example, a change in pressure conditions from domi-

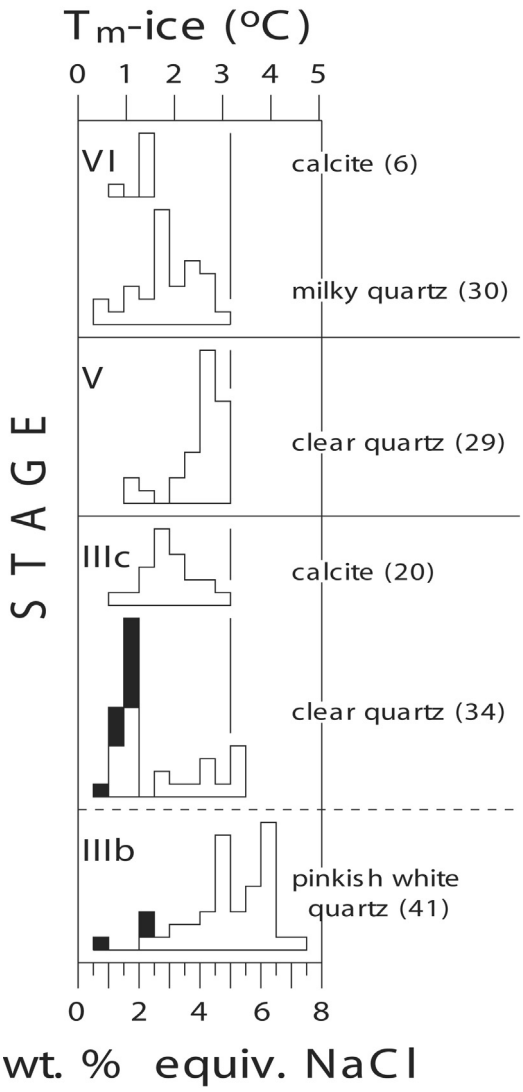

Fig. 5. Histograms of salinities of fluid inclusions in vein minerals of the Mugeuk Au-Ag mine. Data in black are for secondary inclusions; unfilled are for primary + pseudosecondary inclusions. Numbers in parentheses beside mineral names indicate the number of inclusions measured.

nantly lithostatic toward purely hydrostatic could account for about 20°C of this range (Potter, 1977).

However, the much larger ranges of T_h values within each stage (Fig. 4) require an additional explanation. They imply that cooling took place within each stage prior to the onset of the next, indicating that several successive hydrothermal events are responsible for deposition of the complex mineral paragenesis rather than one protracted event. This is supported by textural evidence within the veins. During the main gold-depositing stages, the maximum and average fluid salinities decreased with time (Fig. 5). This indicates that dilution accompanied cooling during gold deposition. The decreases of average fluid salinities during the deposition of quartz and calcite in silver-ore stage V and post-ore stage VI (Fig. 5) also indicate that the hydrothermal system evolved through progressive dilution.

Relationships between homogenization temperatures and salinities for individual stages of the Mugeuk mineral paragenesis (Fig. 6) are also interpreted to indicate overall cooling and dilution of hydrothermal fluids via progressive mixing. However, temperatures and salinities of hydrothermal fluids tend to show renewed increases prior to the onset of each successive mineralization stage, except for the stage V fluid that shows almost the same temperature ranges as for stages IIIc and VI but has slightly higher salinities. The reason of the salinity increase during stage V is not

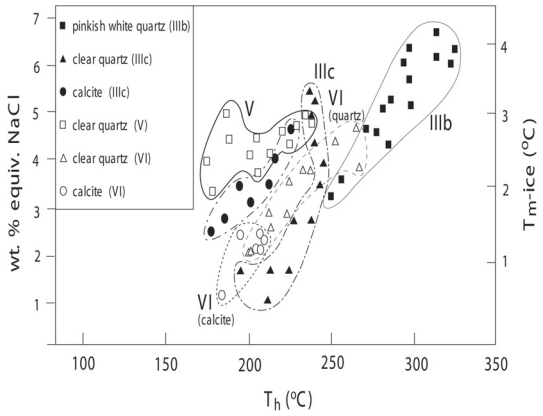

Fig. 6. Plot of homogenization temperature versus salinity for fluid inclusions in vein minerals from the Mugeuk Au-Ag mine. General decreases in temperature and salinity during each stage indicate that mineral deposition was the result of cooling and dilution of ore fluids. Generally renewed higher temperatures and salinities at the start of subsequent stages indicates that ore mineralization was the result of multiple, successive pulses of fluids rather than a single protracted fluid event.

clear. Nevertheless, the resultant *en echelon* pattern on the T_h-salinity plot for most of the mineralization stages can be interpreted to indicate multiple episodes of cooling and dilution throughout the history of the hydrothermal system. This requires successive pulses of hydrothermal fluids for each stage, each of which evolved through cooling and dilution, prior to the introduction of new fluids in the next stage.

A similar pattern was observed for fluids in the Gyeongchang W-Mo-Ag deposits in Korea (So *et al.*, 1991). In that study, temperature and salinity also decreased during each stage of a complex mineral paragenesis. Following cooling and dilution of an earlier stage's fluids, abrupt increases in temperature and salinity of fluids also accompanied the beginning of a new type of vein mineralogy. Such patterns of T_h-salinity are incompatible with a single protracted fluid evolution and require instead a system with multiple periods of fracturing allowing introduction of successive geochemically evolving fluids (So and Yun, 1996).

Geochemical conditions of mineralization

Ranges of temperature and fugacity of sulfur during Au-Ag mineralization were estimated from the phase relations and mineral compositions in the systems Fe-Zn-S and Au-Ag-S (Barton and Toulmin, 1964, 1966), as shown in Figure 7. The mineral composition data used were obtained by us in this study and are available from authors as electronic supplements. Each gold-depositing stage has a unique coexisting mineral assemblage containing sphalerite and electrum: stage II, pyrite + sphalerite (1.6-1.9 mole % FeS) + electrum (52-53 atom. % Ag); stage IIIa, pyrite + sphalerite (3.5 mole % FeS) + chalcopyrite + electrum (49-54 atom. % Ag); stage IIIb, sphalerite (2.1-2.9 mole % FeS) + chalcopyrite + electrum (57-63 atom. % Ag) + galena + argentite; stage IV, sphalerite (1.2-2.2 mole % FeS) + electrum (53-54 atom. % Ag) + galena; stage V, sphalerite (1.6-2.9 mole % FeS) + electrum (75-77 atom. % Ag) + galena + argentite.

These assemblages and chemical compositions indicate the following temperature and log fS_2 conditions for each mineralization stage: stage II, 245° to 257°C and -11.4 to -10.9 atm stage IIIa, 272° to 293°C and -10.7 to -9.7 atm stage IIIb, 222° to 251°C and -13.1 to -11.7 atm stage IV, 233° to 257°C and -11.0 to -11.9 atm stage V, 177° to 199°C and -15.9 to -14.9 atm, respectively.

The overall trend is a gradual decrease in both fS_2 and temperature with time during the gold-mineralizing event (from stage II through IV). These observations are in general agreement with the observed pattern of decreasing average homogenization temperatures for these stages (Fig. 4). While the mineralogically determined temperatures fall within the measured ranges of T_h values for individual paragenetic stages, they typically overlap the lower temperature ends of the ranges. This may be because the ore minerals precipitated during the latter portions of each stage (Fig. 3), following significant earlier fluid cooling and quartz deposition. The good agreement between mineralogical temperature estimates and the lower T_h values for each stage may suggest that the pressure corrections to the T_h values are of the same magnitude. For fluids with salinities of 3-7 wt. % equiv. NaCl, pressure corrections of less than 10-15°C would correspond to pressures of approximately 200-300 bars at temperatures near 250-300°C (Potter, 1977). The pressures of 200-300 bars correspond to approximate depths of 2-3 km and 0.7-1.1 km, assuming purely hydrostatic and lithostatic pressure conditions, respectively.

Large decreases in both fS_2 and temperature followed stage IV and correspond to a shift to silver-rich mineral deposition of stage V. Based on low chlorinities of fluids, gold was likely transported as a bisulfide complex in solution (Seward, 1973). The decreased fS_2 and temperature of the stage V hydrothermal fluids would both have impeded gold transportation. However, chloride-complexed metals such as silver, lead and zinc could continue to have been transported and deposited from the 5 wt. % equiv. NaCl stage V fluids.

Stable isotope study and discussions

In order to elucidate the origin and evolution of hydrothermal fluids of the Mugeuk mine, we measured the $\delta^{34}S$ values of sulfides, $\delta^{13}C$ values of calcite, δ

^{18}O values of vein quartz and calcite, and the δD values of fluid inclusion waters extracted from vein minerals (Tables 1 and 2). Standard techniques for extraction and analysis were used as described by McCrea (1950), Grinenko (1962) and Hall and Friedman (1963). Isotope data are reported in standard δ notation relative to the Canyon Diablo troilite standard for sulfur, the Pee Dee Belemnite standard for carbon, and the V-SMOW for oxygen and hydrogen. The standard error of each analysis is approximately ±0.1‰ for carbon, oxygen and sulfur, and ±2‰ for hydrogen.

Sulfur isotopes

Sulfur isotope data were obtained for 25 hand-picked sulfides from various vein stages (Table 1). It was not possible to separate the tiny, microfracture-hosted stage V sulfide minerals for analysis.

One stage I pyrite had the $\delta^{34}S$ value of 8.0‰. The ranges of $\delta^{34}S$ values of sulfides from other stages were: stage II pyrite, 8.4-10.0‰; stage IIIa arsenopyrite and pyrite, 6.0-8.8‰; stage IIIb sphalerite, chalcopyrite and galena, 4.0-8.4‰; stage IV arsenopyrite, pyrite, sphalerite, chalcopyrite and galena from veins, 2.8-8.1 ‰; stage VI pyrite, 8.0-10.1‰(Table 1). Due to the sequential nature of sulfide precipitation in the veins, there were no useful mineral pairs for calculation of equilibrium isotope temperature.

Based on the fluid inclusion homogenization temperatures in associated quartz, the following $\delta^{34}S$ values of H_2S were calculated for each stage using the sulfur isotope fractionation equations in Ohmoto and Rye (1979): stage I, 6.8‰; stage II, 7.2-8.8‰; stage IIIa, 5.0-7.0‰; stage IIIb, 6.3-8.5‰; stage IV, 4.5-6.0‰; stage VI, 6.6-8.7‰. The calculated $\delta^{34}S_{H2S}$ values show small variations over the ore deposition temperature range of 250° to 350°C. This may reflect the dominance of H_2S in the ore fluids. A temperature decrease (up to 100°C) would have little effect on the $\delta^{34}S_{H2S}$ values of a fluid if its sulfur were dominantly H_2S (Ohmoto and Rye, 1979). Therefore, the $\delta^{34}S_{H2S}$ values (4.5 to 8.8‰) may be taken as an approximation of the total sulfur isotope composition of the entire hydrothermal fluid. The host Jurassic granitic rocks are one potential source for sulfur with a $\delta^{34}S$ as high as 9‰ (Shelton *et al.*, 1988; So *et al.*, 1989), though contributions from Cretaceous granitic and sedimentary rocks cannot be eliminated.

Table 1. Sulfur isotope data for vein sulfides from the Mugeuk Au-Ag mine

Stage	Sample no.	Mineral	$\delta^{34}S$ (‰)	T (°C)[a]	$\delta^{34}S_{H2S}$ (‰)[b]
I	MK-C	Pyrite	8.0	300	6.8
II	MK-1	Pyrite	8.4	300	7.2
II	MK-2	Pyrite	9.3	300	8.1
II	MK-3	Pyrite	10.0	300	8.8
II	MK-4	Pyrite	9.7	300	8.5
IIIa	MK-9	Arsenopyrite	8.8	-	-
IIIa	MK-32	Pyrite	7.7	350	6.7
IIIa	MK-1873	Pyrite	7.6	350	6.6
IIIa	MK-L37	Pyrite	8.0	350	7.0
IIIa	MK 9710	Pyrite	6.0	350	5.0
IIIb	MK-5	Galena	4.0	250	6.3
IIIb	MK-6	Sphalerite	8.4	270	8.1
IIIb	MK-7	Sphalerite	8.2	270	7.9
IIIb	MK-8	Chalcopyrite	8.3	270	8.5
IIIb	MK 97A	Galena	5.0	250	7.3
IV	MK-10	Arsenopyrite	8.1	-	-
IV	MK-24	Sphalerite	5.7	250	5.3
IV	MK-24A	Pyrite	6.3	270	4.9
IV	MK-24B	Sphalerite	4.9	250	4.5
IV	MK-F1	Sphalerite	5.2	250	4.8
IV	MK-F2	Pyrite	6.4	270	5.0
IV	MK-G	Galena	2.8	250	5.1
IV	MK-T	Chalcopyrite	5.8	270	6.0
VI	MK-11	Pyrite	10.1	270	8.7
VI	MM-27	Pyrite	8.0	270	6.6

[a] Based on fluid inclusion and/or thermodynamically estimated temperatures

[b] Calculated sulfur isotope compositions of H_2S, based on fractionation equations in Ohmoto and Rye (1979)

Carbon and oxygen isotopes

The $\delta^{13}C$ and $\delta^{18}O$ values for vein minerals and their inclusion fluids are summarized in Table 2. Because of the difficulty of recognizing and separating stage V quartz from microfractures and tiny veinlets, only one sample was analyzed for its $\delta^{18}O$ value.

The two $\delta^{18}O$ values of chalcedonic quartz from stage I are both 5.6‰. We have no temperature constraints for this earliest pre-ore mineralization, but believe it represents a cooler event, unrelated to later ore-depositing stages II through V. The $\delta^{18}O$ values of vein quartz from gold-ore stages II through IIIc range from 9.5 to 6.7‰. The $\delta^{18}O$ values of vein quartz from stage IV and silver-rich stage V are 5.6 to 5.7‰. Those of post-ore stage VI quartz are 2.5 to 3.0‰. Though there are only 23 analyzed quartz samples, their $\delta^{18}O$ values indicate a trend toward lower values with increasing paragenetic time during the mineralizing event. The values do not decrease gradually, but decrease abruptly after stage III, following major gold

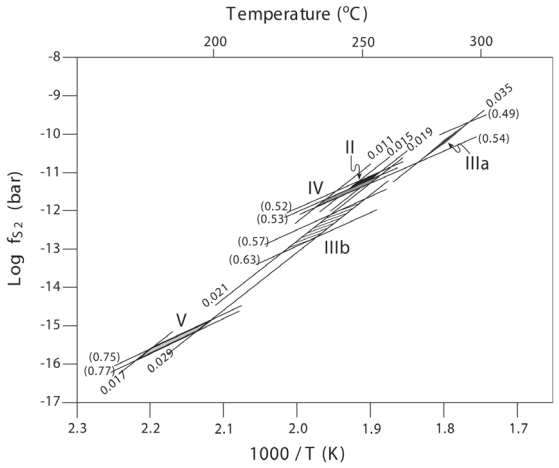

Fig. 7. Sulfur fugacity versus temperature diagram showing sulfidation reactions pertinent to Mugeuk mineral assemblages. Sulfur fugacity and temperature decrease systematically from stage II through IV, with a large decrease toward stage V. These decreases are interpreted to represent repeated incursions of meteoric waters into the hydrothermal system, with stage V representing the dominance of unevolved meteoric waters as the hydrothermal system waned. Numbers in parenthesis are the atomic fraction of silver in electrum; numbers without parentheses are the mole fraction of FeS in sphalerite.

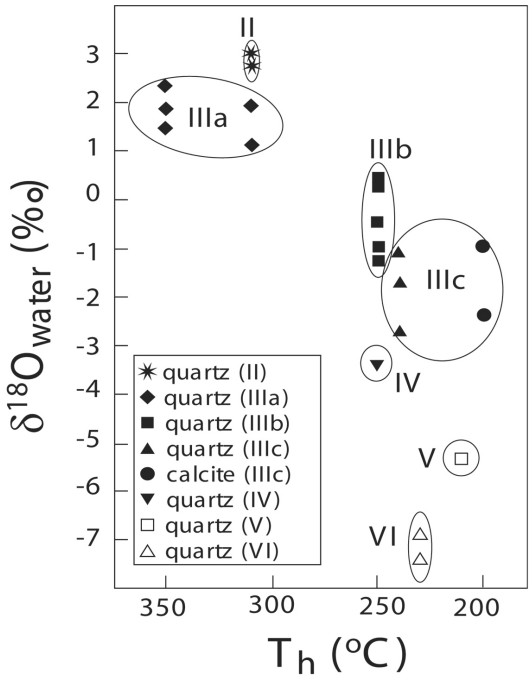

Fig. 8. T_h versus $\delta^{18}O_{water}$ values showing systematic decreases of $\delta^{18}O_{water}$ value with decreasing age at the Mugeuk mine. These data reflect the progressive dominance of isotopically less evolved meteoric waters in the hydrothermal system.

deposition.

Using the quartz-water oxygen isotope fractionation equation of Matsuhisa et al. (1979) and a best estimate of temperature for each sample based on fluid inclusions in that portion of the sample used for isotope analysis, the calculated equilibrium oxygen isotope compositions of waters in the hydrothermal ore fluids are: stage II, 3.0 to 2.8‰; stage IIIa, 2.4 to 1.2 ‰; stage IIIb, 0.4 to -1.3‰; stage IIIc, -1.2 to -2.7‰; stage IV, -3.3‰; stage V, -5.3‰; stage VI, -6.9 to -7.4 ‰. Variations of ±20°C in the temperatures used for the calculations would result in changes in the calculated water values of ±0.6‰.

There is an apparent decrease in $\delta^{18}O_{water}$ values with decreasing age, as recognized in the $\delta^{18}O_{quartz}$ values. However, within the main gold-depositing stage of the paragenesis, the decrease in $\delta^{18}O_{water}$ values is more pronounced than that of the $\delta^{18}O_{quartz}$ values themselves because of the effect of generally decreasing temperature during stage III (Figs. 4 and 8).

The $\delta^{13}C$ and $\delta^{18}O$ values of calcite from gold-ore stage IIIc are -4.9 and -5.1‰, and 7.2 and 8.7‰, respectively. Using the calcite-water oxygen isotope fractionation equation of Friedman and O'Neil (1977), coupled with temperature estimates based on fluid inclusions, the $\delta^{18}O$ values of waters in equilibrium with the calcites are -0.9 to -2.4‰. These $\delta^{18}O_{water}$ values agree well with those calculated from paragenetically earlier stage IIIc quartz (-1.2 to -2.7‰).

Hydrogen isotopes

Fluid inclusion waters were extracted by crushing vein quartz and calcite samples, and these were analyzed for their hydrogen isotope compositions (Table 2). Veinlets of stage V quartz were too small to obtain enough fluid to analyze. The δD values of inclusion waters from all stages analyzed range from -85 to -66 ‰ (Table 2). Individual stages have similar ranges.

Although we chose samples for analysis that contained as few secondary inclusions as possible, we may have analyzed more than one generation of primary and

Table 2. Carbon, oxygen and hydrogen isotope data for quartz, calcite and chalcedony and their inclusion fluids, Mugeuk Au-Ag mine

Stage	Sample no.	Mineral	$\delta^{13}C$ (‰)	$\delta^{18}O$ (‰)	T (°C)[a]	$\delta^{18}O_{water}$ (‰)[b]	δD (‰)
I	MK-C1	Chalcedony		5.6	300	−0.8	
I	MK-W	Chalcedony		5.6	300	−0.8	-
II	MK-33A	Quartz		9.3	310	2.8	−66
II	MK-C2	Quartz		9.5	310	3.0	−78
IIIa	MK-18	Quartz		7.1	350	1.8	−73
IIIa	MK-32	Quartz		8.8	300	1.9	−69
IIIa	MK-36	Quartz		8.0	300	1.2	−72
IIIa	MK-1873	Quartz		7.7	350	2.4	−75
IIIa	MK-97C	Quartz		6.8	350	1.5	−72
IIIa	MK-33B	Quartz		9.2	250	0.3	−67
IIIb	MK-P	Quartz		7.9	250	−1.0	-
IIIb	MK-Q1	Quartz		9.3	250	0.4	−73
IIIb	MK-1	Quartz		7.6	250	−1.3	−69
IIIb	MK-97B	Quartz		8.4	250	−0.5	−85
IIIb	MK-27	Quartz		8.2	240	−1.2	−67
IIIc	MK-31	Quartz		7.6	240	−1.8	−71
IIIc	MK-D1	Quartz		6.7	240	−2.7	−76
IIIc	MK-A	Calcite	−5.1	7.2	200	−2.4	−79
IIIc	MK-B	Calcite	−4.9	8.7	200	−0.9	−81
IV	MK-D2	Chalcedony		5.6	250	−2.9	-
V	MK-V	Quartz		5.7	210	−5.3	-
VI	MK-2	Quartz		3.0	230	−6.9	−71
VI	MK-30	Quartz		2.5	230	−7.4	−84

[a] Based on fluid inclusion and thermodynamically estimated temperatures and paragenetic constraints

[b] Calculated oxygen isotope compositions of water in equilibrium with minerals, based on fractionation equations as follows: Matsuhisa et al. (1979) for quartz−water; Kita et al. (1985) for chalcedony−water; and Friedman and O'Neil (1977) for calcite−water. Fractionation between chalcedony and water is assumed to be the same as for that between amorphous silica and water

pseudosecondary inclusion fluids. This may, in part, account for the similarities of δD values for all stages. Alternatively, the similarity in δD values could indicate that the δD values of local meteoric waters at the time of mineral deposition in the various stages of the paragenesis were similar. Studies of other Cretaceous gold-silver deposits in Korea have shown that the δD values of local meteoric waters at the time of ore mineralization were commonly between -65 and -85‰ (Taylor, 1997). Modern meteoric waters and hot spring waters in South Korea have δD values of -45 to -75‰ (Kim and Nakai, 1981). The overlap of these ranges of δD values with those of magmatic waters and highly exchanged meteoric waters negates unique interpretations based on hydrogen isotopes. In our study, variations of $\delta^{18}O$ values of hydrothermal fluid with time may prove to be more useful in elucidating the history of fluid-rock interactions in the Mugeuk hydrothermal system.

Interpretation of O-H isotope data and discussion on ore genesis

The calculated $\delta^{18}O_{water}$ values systematically decrease with decreasing age (Fig. 8), and we interpret this trend to indicate successive introduction of isotopically less-evolved meteoric waters into the Mugeuk hydrothermal system. Through time during the mineralizing events, the hydrothermal system became more open to meteoric waters that were progressively less equilibrated with igneous host rocks. Variations of ±20°C in the temperatures chosen for calculations would result in changes in the estimated water values of ±0.6‰, but they would have no effect on the overall topology of Figure 8.

From gold-silver ore stages II through IV, $\delta^{18}O_{water}$ values decrease gradually from +3‰ toward 3‰ as temperatures decrease from about 350° to <250°C (Fig. 8). We interpret this trend to indicate the introduction of new pulses of ore fluids, each of which equilibrated isotopically with the host granitic rocks at successively higher water-to-rock ratios and lower temperatures. Gradually the host rock would have lost its ability to effectively buffer the oxygen isotope composition of the hydrothermal fluids.

Following the gold-silver stages, there is apparently an abrupt 2.5‰ decrease in $\delta^{18}O_{water}$ values at nearly constant temperature that corresponds to the shift in mineralogy to silver-base metal deposition of stage V and post-ore stage VI (Fig. 8). We interpret this shift to indicate the dominance of isotopically less evolved meteoric waters during the waning stages of the Mugeuk hydrothermal system. Even though progressively larger amounts of cooler meteoric waters caused the cessation of gold deposition, the elevated salinities of stage V fluids (about 3.5 to 5 wt. % equiv NaCl) may have enabled the continued transport and deposition of silver and base metals as chloride complexes. By the start of economically barren stage VI, $\delta^{18}O_{water}$ values decreased to below -7‰, marking the final incursion of waters with end-member meteoric isotopic signatures into the Mugeuk hydrothermal system.

Figure 9 shows the distribution of measured and calculated $\delta^{18}O_{water}$ and δD_{water} values for Mugeuk on a conventional plot of H versus O isotopic values. The data display a classic $\delta^{18}O$ shift (Taylor, 1974), indicating the fluids exchanged oxygen isotopes with the host granitic rocks of Jurassic age at elevated temperatures. With time, fluid compositions approached the meteoric water line as water-to-rock ratios increased and the host granitic rocks lost their ability to buffer the oxygen isotope compositions of the hydrothermal fluids of Late Cretaceous age. Similar patterns have been documented in many other Korean granite-related

Au-Ag deposits as well as in a variety of other epithermal vein deposits worldwide (Taylor, 1997).

The $\delta^{18}O_{water}$ and δD_{water} values of the Mugeuk deposits are most similar to those of Korean-type (approximately 1.25 km deep) gold-silver deposits (Taylor, 1997). Notable differences are: the Mugeuk data extend to lower $\delta^{18}O_{water}$ values than most Korean-type deposits; and the mineralogy and mineral paragenesis of the Mugeuk deposits are more complicated. The mineralogy is more similar to shallower, silver-rich epithermal deposits such as the Tongyeong Ag-Te mine in Korea (Shelton *et al*., 1990) and numerous epithermal deposits worldwide (Casadevall and Ohmoto, 1977).

Thus, we consider Mugeuk deposits as products of a complex hybrid system. Early stages of the Mugeuk hydrothermal history involved successive introduction of progressively less evolved meteoric waters during deposition of gold-silver mineralization. Later stages were the result of inundation of the hydrothermal system by episodic introduction of isotopically unevolved meteoric waters, resulting in a silver-rich epithermal overprint on the earlier gold-silver system.

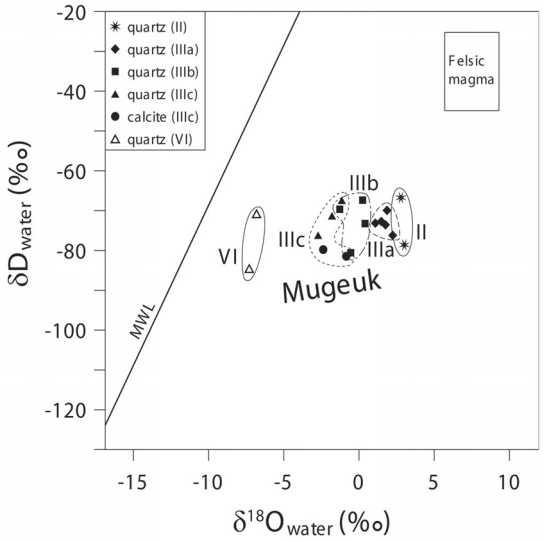

Fig. 9. Hydrogen versus oxygen isotope plot for hydrothermal fluids from the Mugeuk mine. The 'felsic magma' box indicates the isotopic range of water degassed from felsic magmas in equilibrium (Taylor, 1986) and the meteoric water line (MWL) is from Craig (1961). The data show a classic ^{18}O shift (Taylor, 1974, 1997) indicating progressive dominance of less evolved meteoric waters in the hydrothermal system.

References

Barton, P. B., Jr. and Toulmin, P., III. , 1964, "The electrum tarnish method for determination of the fugacity of sulfur in laboratory sulfide systems", *Geochimica Cosmichimica Acta*, Vol. 28, pp. 619-640.

Barton, P. B., Jr. and Toulmin, P., III. , 1966, "Phase relations involving sphalerite in the FeZnS system." *Economic Geology*, Vol. . 61, pp. 815-849.

Bodnar, R. J., 1993, "Revised equation and table for determining the freezing point depression of H2ONaCl solutions." *Geochimica Cosmichimica Acta*, Vol. 57, pp. 683-684.

Casadevall, T. and Ohmoto, H., 1977, "Sunnyside mine, Eureka mining district, San Juan County, Colorado. Geochemistry of gold and base metal formations in the volcanic environment." *Economic Geology*, Vol. 72, pp. 12851320.

Cheong, C. H., Park, Y. A. and Kim, H. M., 1976, Geological map (1:50,000) of Korea: Eumseong quadrangle. Korean Institute of Geology and Mineral Resources

Craig, H., 1961, "Isotopic variations in meteoric waters." *Science*, Vol. 133, pp. 17021703.

Friedman, I. and O'Neil, J. R., 1977, "Compilation of stable isotope fractionation factors of geochemical interest." In: Fleisher, M. (ed) Data of geochemistry (6th ed). *USGS Professional Paper* Vol. 440KK, pp. 412.

Grinenko, V. A., 1962, "Preparation of sulfur dioxide for isotopic analysis." *Zeitschrift Neorganische Khimii* Vol. 7, pp. 2478-2483.

Hall, W. E. and Friedman, I., 1963, "Composition of fluid inclusions, Cave-in-Rock fluorite district, Illinois and upper Mississippi Valley zinclead district." *Economic Geology*, Vol. 58, pp. 886-911.

Kim, K. H. and Nakai, N., 1981, "A study on hydrogen, oxygen and sulfur isotopic ratios of the hot spring waters in South Korea." *Geochemistry (Japan)*, Vol. 15, pp. 616.

Kim, K. H., Kim, O. J. and Chang, W. S. , 1990, "Stable isotope and fluid inclusion studies of the Mugug AuAg mineral deposits (in Korean)." *Korean Institute Mining Geology Journal,* Vol. 23, pp. 19.

Kim, O. J., 1987, Chapter 10: Tectonic provinces. In: Lee, D. S. (ed.), Geology of Korea. *Geological Society of Korea*, pp. 237-252.

Kita, I., Taguchi, S. and Matsubaya, O., 1985, "Oxygen isotope fractionation between amorphous silica and water at 3493°C." *Nature*, Vol. 314, pp. 83-84.

Lee, M. S. , 1981, "Geology and metallic mineralization associated with Mesozoic granitic magmatism in South Korea." *Mining Geology*, Vol. 31, pp. 235-244.

Matsuhisa, Y., Goldsmith, J. R. and Clayton, R. N. , 1979, "Oxygen isotope fractionation in the system quartzalbiteanorthitewater." *Geochimica Cosmochimica Acta*,

Vol. 43, pp. 1131-1140.
McCrea, J. M. , 1950, "The isotope chemistry of carbonates and a paleotemperature scale." *Jounal of Chemical Physics*, Vol. 18, pp. 849-857.
Ohmoto, H. and Rye, R. O. , 1979, Isotopes of sulfur and carbon. In: Barnes, H. L. (ed) *Geochemistry of Hydrothermal Ore Deposits (2nd ed)*, New York, Wiley Intersci., pp. 509-567.
Park, H. I. and Kang, S. J. , 1988, "Gold and silver mineralization of Samhyungje vein, the Mugeug mine" *Korean Insitute Mining Geology Journal* Vol. 21, pp. 257-268.
Potter, R. W. III., 1977, "Pressure corrections for fluid-inclusion homogenization temperatures based on the volumetric properties of the system NaCl-H_2O." *United States Geological Survey Journal Research*, Vol. 5, pp. 603-607.
Roedder, E., 1984, Fluid inclusions. *Review in Mineralogy* Vol. 12, pp. 644.
Seward, T. M., 1973, "Thio complexes of gold and the transport of gold in hydrothermal ore solutions." *Geochimica Cosmochimica Acta* Vol. 37, pp. 379-399.
Shelton, K. L. and Orville, P. M., 1980, "Formation of synthetic fluid inclusions in natural quartz." *American Mineralogist*, Vol. 65, pp. 1233-1236.
Shelton, K. L., So, C. S. and Chang, J. S., 1988, "Gold-rich mesothermal vein deposits of the Republic of Korea: geochemical studies of the Jungwon gold area." *Economic Geology*, Vol. 83, pp. 1221-1237.
Shelton, K. L., So, C. S., Haeussler, G. T., Chi, S. J. and Lee, K. Y., 1990, "Geochemical studies of the Tongyoung goldsilver deposits, Republic of Korea: evidence of meteoric water dominance in a Te-bearing epithermal system." *Economic Geology*, Vol. 85, pp. 1114-1132.
Shimazaki, H., Lee, M. S., Tsusue, A. and Kaneda, H., 1986, "Three epochs of gold mineralization in South Korea." *Mining Geology*, Vol. 36, pp. 265-272.
Shin, Y. W. and Suh, K. S., 1987, "Exploration and development of the Muguk Au mine (in Korean)." *Korean Insitute Mining Geology Journal*, Vol. 20, pp. 261- 271.
So, C. S. and Yun, S. T., 1996, "Geochemical evidence of progressive meteoric water interaction in epithermal AuAg mineralization, JeongjuBuan district, Republic of Korea." *Economic Geology* Vol. 91, pp. 636-646.
So, C. S., Chi, S. J., Yu, J. S. and Shelton, K. L., 1987, "The Jeoneui goldsilver mine, Republic of Korea: a geochemical study." *Mining Geology*, Vol. 37, pp. 313- 322.
So, C. S., Shelton, K. L., Chi, S. J. and Yun, S. T., 1991, "Geochemical studies of the Gyeongchang WMo mine, Republic of Korea: progressive meteoric water inundation of a magmatic hydrothermal system." *Economic Geology*, Vol. 86, pp. 750-767.
So, C. S., Yun, S. T. and Shelton, K. L., 1995, "Mesothermal gold vein mineralization of the Samdong mine, Youngdong mining district, Republic of Korea." *Mineralium Deposita*, Vol. 30, pp. 384-396.
So, C. S., Yun, S. T., Choi, S. H. and Shelton, K. L., 1989, "Geochemical studies of hydrothermal goldsilver deposits, Republic of Korea: Yangdong mining district." *Mining Geology*, Vol. 39, pp. 919.
Sugaki, A., Kim, O. J. and Kim, W. J. , 1986, "Gold and silver ores of the Geumwang mine in South Korea and their mineralization." *Mining Geology*, Vol. 36, pp. 555- 572.
Taylor, B. E., 1986, Magmatic volatiles: isotopic variations of C, H and S. In: *Reviews in Mineralogy, Volume 16.* Mineralogical Society of America., pp. 185-219.
Taylor, H. P., Jr., 1974, "The application of oxygen and hydrogen isotope studies to problems of hydrothermal alteration and ore deposition." *Economic Geology*, Vol. 69, pp. 843-883.
Taylor, H. P., Jr., 1997, Oxygen and hydrogen isotope relationships in hydrothermal mineral deposits. In: Barnes, H. L. (ed) *Geochemistry of Hydrothermal Ore Deposits (3rd ed).* New York, Wiley, pp. 229-302.
Tsusue, A., Mizuta, T., Watanabe, M. and Min, K. G., 1981, "Jurassic and Cretaceous granitic rocks in South Korea." *Mining Geology*, Vol. 31, pp. 1261-1280.
Yang, S. Y. and Chang, K. H. (1987) Chapter 6: Mesozoic Erathem. In: Lee, D. S. (ed.), *Geology of Korea.* Geological Society of Korea, pp. 157-201.
Yun, S. T., So, C. S., Choi, S. H., Shelton, K. L. and Koo, J. H., 1993, "Genetic environments of germanium- bearing goldsilver vein ores from the Wolyu mine, Republic of Korea." *Mineralium Deposita*, Vol. 28, pp. 107-121.

허 철 호
1990년 2월 고려대학교 이과대학 지질학과 학사
1992년 2월 고려대학교 이과대학 지질학과 석사
2001년 2월 고려대학교 이과대학 지구환경과 박사

현재 국립공원관리공단 국립공원연구소 책임연구원
(E-mail; chheo@npa.or.kr)

이 재 호
1985년 2월 고려대학교 이과대학 지질학과 학사
1987년 8월 고려대학교 이과대학 지질학과 석사
1993년 2월 고려대학교 이과대학 지질학과 박사

한국지질자원연구원 지질기반정보연구부 선임연구원
(E-mail; jhlee@kigam.re.kr)